IEEE Access
Multidisciplinary | Rapid Review | Open Access Journal

Date of publication xxxx 00, 0000, date of current version xxxx 00, 0000.

Digital Object Identifier 10.1109/ACCESS.2024.Doi Number

Global Navigation Satellite System Positioning under Interference Conditions

Sebastián Čikovský [1], Member, IEEE, Milan Džunda [2]

[1]Faculty of Aeronautics, Technical University of Kosice, Department of Air Transport Management, 04001, Kosice
[2]Faculty of Aeronautics, Technical University of Kosice, Department of Air Transport Management, 04001, Kosice

Corresponding author: First S.Č. Author (e-mail: sebastian.cikovsky@tuke.sk).

ABSTRACT This paper contains a model of the flying object (FO) flight trajectory in the geocentric coordinate system and a model of FO position measurement errors using a Global Navigation Satellite System (GNSS) receiver under interference conditions. The size of the FO coordinate errors in the horizontal and vertical planes ranged from +20.0 m to -20.0 m. This paper's contribution is the creation of algorithms for processing GNSS signals under interference conditions based on the Savitzky-Golay filter and neural network. The simulation results confirmed that the Savitzky-Golay filter when applied in the GNSS receiver, can suppress FO position measurement errors. For example, if absolute FO position measurement errors due to GNSS interference were from 0.0 m to 5.0 m, and the mean square error of these errors was 0.441 m^2, the Savitzky-Golay filter reduced them to a value from 0.0 m to 0.8 m, and the mean square error of these errors was equal was 0.0195 m^2. In this case, the mean error value in the FO position after filtering with the Savitzky-Golay filter was 0.32 m, and the mean square error was 0.019 m^2. Advanced machine learning techniques in the form of neural networks were also used to suppress errors from the output of the Savitzky-Golay filter. The simulation confirmed that if the FO position errors at the neural network's input ranged from 0 m to +0.8 m, the neural network reduced them to 0.0 m to 0.5 m. The mean FO position error value was 0.12 m, and the mean square error was 0.0089 m^2. The results of this study may contribute to more precise and reliable FO navigation and improve the use of GNSS systems in interference conditions.

INDEX TERMS *GNSS, Interference, Trajectory, Filtering, Neural network*

I. INTRODUCTION

Satellite navigation systems such as Galileo and GPS provide critical data on the position of FO and time. This data is essential for air traffic management and safety. In actual conditions, FO position data is affected by various types of interference. These factors may cause inaccuracies, which need to be minimised to ensure a smooth and safe flow of air traffic. Our research addressed the accuracy issues of determining the FO flight trajectory, which GNSS (Global Navigation Satellite System) measured. Signal filtering and machine learning methods were used to improve the accuracy of flight trajectory tracking. The influence of jamming, filtering techniques and machine learning has been the subject of several foreign studies, which we present in the following text.

The authors [1, 2] analysed the performance of dual-frequency positioning in the Galileo system and the accuracy of different GNSS receivers. They found that professional receivers achieve the highest accuracy. Study [3] presents the effect of satellite constellation on GNSS accuracy and the optimization of the constellation to provide users with maximum accuracy and coverage. The accuracy and reliability of the Galileo HAS service have been evaluated in [4]. The research showed that the HAS service significantly improves positioning accuracy and signal reception reliability. Techniques to mitigate interference in GNSS, including an adaptive filter and robust methods to suppress it, are presented in [5, 6]. The impact of these techniques on the accuracy of measurements and positioning using real data under interference conditions is evaluated. Improving GNSS positioning accuracy by combining data from multiple GNSS devices is addressed by the authors of [7]. The study shows that this approach can significantly improve positioning accuracy. The authors of [8] investigate how meaconing affects GNSS receivers. According to the authors, meaconing can create a multipath environment in which the delayed signals appear as legitimate satellite signals. Simulations show that meaconing decreases the signal-to-noise ratio, reducing GNSS accuracy. The impact of spoofing on the accuracy and reliability of GNSS receivers of different levels is analysed in [9], identifying their vulnerabilities and suggesting ways to mitigate the risks. In [10], how out-of-band interference affects GNSS receivers is defined, including the effects on sensitivity and accuracy. Different interference mechanisms are analysed, and mitigation techniques are proposed.

The impact of intentional GNSS radio interference is investigated in [11, 12, 13]. The authors analyse various sources of interference and their effects on receiver performance, proposing methods to mitigate these adverse effects. The authors of [14] combine the wavelet transform with the Hough transform to improve the detection capability of frequency-modulated interference signals. The GNSS anti-jamming method based on the fractional Fourier transform represents an effective anti-jamming detection and mitigation technique for GNSS receivers [15]. Researchers propose the use of fractional Fourier transform for the identification and suppression of interfering signals. The impact of GNSS interference on air traffic in Eastern Europe is presented in [16]. Based on data from the OpenSky Network, days when more than 1000 flights were affected by interference were identified. The results show that interference is more frequent at higher flight level.

II. Selected knowledge from applying digital filtering and neural networks to suppress GNSS interference

A study [17] provides an overview of GNSS interference and examines the use of neural networks to mitigate it. Intentional and unintentional jamming is analysed, with an emphasis on jamming and an evaluation of existing jamming suppression techniques. A system for monitoring, detecting and classifying GNSS jamming is presented in [18]. It uses commonly available hardware and machine learning to process GNSS measurement signals. It enables accurate real-time interference detection and classification. Machine learning and crowdsourcing data from Android smartphones are used for monitoring, classification of GNSS interference, reliable detection and localization of interference sources [19]. Using the U-Net deep learning architecture, the system achieves more than 90% accuracy in identifying six types of interference and enables localization with an error of less than 2.5 meters. EUROCONTROL has conducted a GNSS Receiver Interference Testing study to better understand the behavior of currently fielded aircraft GNSS receivers when subject to interference. Based on the simulation results, a set of interference detection techniques have been defined and tested using Support Vector Machine method and Random Sample Consensus method [20].

A deep neural network-based approach for classifying interference and jammers in GNSS systems effectively identifies different types of interference [21]. This model improves the interference robustness of GNSS receivers, which can contribute to higher reliability and accuracy in real-world conditions. GNSS signal interference in aviation is detected using machine learning and ADS-B data. Neural networks enable the identification and localization of interference sources [22]. The models presented in this study allow us to achieve high positioning accuracy. A specific preprocessing has been developed for data processing. The interference detection and localization method in GNSS applications presented in [23] combines the analysis of signals from multiple receivers with advanced machine learning algorithms. This approach allows us to localize interference sources and identify their characteristics efficiently. In [24], the improvement of GNSS measurement accuracy through digital filtering is addressed by applying a Savitzky-Golay filter. Compared to the Kalman filter, this approach is characterized by lower computational complexity and high efficiency in GNSS signal interference conditions. The improvement of the frequency response of Savitzky-Golay filters using colour noise models is addressed in [25]. The authors propose to adapt the filters to specific spectral characteristics of the noise, thus increasing their accuracy and applicability in processing signals with complex spectral variability. The results show that this method extends the capabilities of Savitzky-Golay filters in digital signal processing.

The authors [26] proposed an algorithm to improve the accuracy of aircraft positioning using DGPS and multiple GNSS reference stations. They employed a weighting model based on baseline length, vector length error, and the number of observed satellites. Flight experiments confirmed a significant improvement in accuracy in ellipsoidal coordinates. The accuracy of aircraft positioning using dual GPS receivers was analyzed in [27]. Their modified algorithm, which uses weighted measurements, enabled a significant improvement in horizontal coordinates (62 to 91%) and in the vertical component (16 to 83%). The data were obtained from real flight experiments conducted in the vicinity of the military airfield in Dęblin, demonstrating the practical applicability of this methodology for validating GNSS techniques in aerial navigation.

Our research focused on suppressing errors in measuring the position of a flying object using a GNSS system operating in interference conditions. To increase the resistance of the GNSS receiver to interference, a Savitzky-Golay filter and a neural network were used. These methods can efficiently reconstruct the original FO flight trajectory even with significant interference, which is crucial for aviation navigation systems and other mission-critical applications. The results of this study can contribute to more accurate and reliable navigation and enhance the use of GNSS systems, such as Galileo, in interference conditions. The flight simulation was performed in the MATLAB programming environment.

III. Methodology

We assumed that the GNSS system measures the position of the FO at specified times, and based on these measurements, the trajectory of the FO flight can be determined. For this purpose, we created a model of the FO flight trajectory in the geocentric coordinate system for the case where the receiver accurately measures the FO's position.

A. Model of the flight trajectory of a flying object

The initial point of the flight trajectory was located over the Košice airport. This model contained parameters of accurate FO flight such as latitude, longitude, altitude and airspeed. The geodetic coordinates of the aircraft were subsequently transformed into geocentric X, Y and Z coordinates, which are more suitable for the analysis of positional accuracy. In creating the flight model, initial geographical coordinates in the form of latitude, FO longitude and altitude are assigned at the origin of the FO. In this case, the initial position of the FO was defined using the latitude and FO longitude for the Kosice area, namely latitude 48.6630∘ and longitude 21.2415∘. The flight takes over 20 minutes, hence time t∈ [0,1200] seconds. The flight altitude is 10,000 metres, which corresponds to the stabilised flight level of the FO. The FO flight model considers that FO flies at a constant speed of 800 km.h^{-1}, 222.22 m.s^{-1}. FO flies along a curved trajectory, which is a left-hand turn. The change in the longitude of FO's centre of gravity is calculated based on the distance flown, and alterations in longitude are adjusted to the magnitude of the curvature of the Earth at that point. The latitudinal turn is modelled using a sinusoidal function with an amplitude of 0.01 radians and a minimal frequency of 0.0015 s^{-1}.

We considered this trajectory a reference and used it to evaluate the accuracy of the designed GNSS receiver, which measured the FO position under interference conditions. The simulated FO trajectory is shown in the geocentric coordinate system, where X, Y and Z represent the FO coordinates in meters. The FO speed is equal:

To calculate the curvature of the Earth, we use an ellipsoidal model of the Earth, where the semi-major axis a=6378137 m and the eccentricity e=0.08181919. We calculate the radius of curvature by:

$$N = \frac{a}{\sqrt{1 - e^2 sin^2(latitude)}} \quad (1)$$

The longitude of the FO centre of gravity varies with time and speed as follows:

$$\text{longtitude}(t) = \text{initial}_{FOn} + \frac{v \,.\, t}{N \,.\, cos(initial_{lat})} \quad (2)$$

The latitude position of the FO centre of gravity was modelled as follows:

$$\text{Latitude}(t) = \text{initial}_{lat} + A \,.\, \sin(0.0015 \,.\, t), \quad (3)$$

where amplitude A=0.01 rad. The curve is modelled by the sine function sin (0.0015.t).

To calculate the geocentric coordinates, we used relationships that consider the elevation and curvature of the Earth at our specified location:

$$X(t) = (N + \text{altitude}).\cos(\text{latitude}(t)).\cos(\text{longitude}(t)) \quad (4)$$
$$Y(t) = (N + \text{altitude}).\cos(\text{latitude}(t)).\sin(\text{longitude}(t)) \quad (5)$$
$$Z(t) = (N\,(1 - e^2) + \text{altitude}).\sin(\text{latitude}(t)) \quad (6)$$

The simulation results of the FO trajectory are shown in Figure 1.

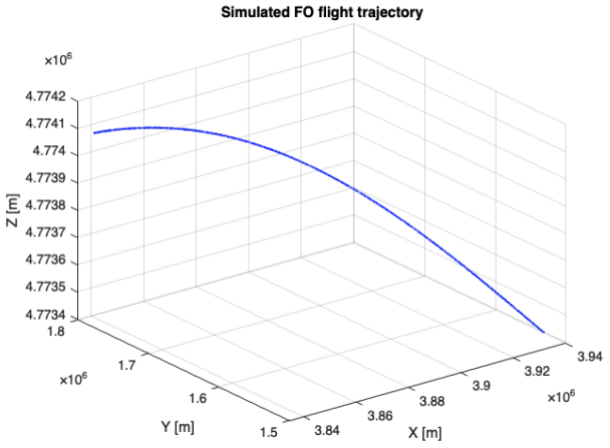

FIGURE 1. Simulated FO flight trajectory

The flight trajectory represents a curvilinear flight with a left-hand turn. This trajectory would be measured by the GNSS receiver if it accurately determined the FO's position. In actual conditions, the GNSS signals are interfered with by unintentional and intentional interference, which causes errors in the FO flight trajectory measurement. Therefore, we supplemented the flight trajectory model with a model of errors in flight trajectory measurement.

B. Model of errors in measuring the flight trajectory of a flying object

This model considers the errors caused by interference, atmospheric effects, and system effects on the accuracy of the FO position measurement by GNSS systems. The flight trajectory measurement errors ΔX,ΔY, and ΔZ were generated at each simulation step for each FO X, Y, and Z position coordinated by random number generators in the MATLAB programming environment.

The flight trajectory measurement errors ΔX, ΔY, and ΔZ were generated by random number generators in MATLAB, each configured to produce normally distributed (Gaussian) errors with a mean μΔ of 0 and a variance σ² of 1. In the simulation, the size of the errors was varied using the constant k:

$$\Delta X = k.\Delta_{X(g)}, \quad (7)$$
$$\Delta Y = k.\Delta_{Y(g)}, \quad (8)$$
$$\Delta Z = k\,\Delta Z_{(g)}, \quad (9)$$

where the constant k was used to change the value of the generated error.

We then added the generated coordinate errors to the corresponding X, Y and Z coordinates:

$$X_{er} = X + \Delta X \quad (10)$$
$$Y_{er} = Y + \Delta Y \quad (11)$$
$$Z_{er} = Z + \Delta Z. \quad (12)$$

In this way, we obtained inaccurate data on the FO position corresponding to the data from the GNSS receiver's output.

We determined the FO ΔP positioning error by equation:

$$\Delta P = (\Delta X^2 + \Delta Y^2 + \Delta Z^2)^{0.5} \quad (13)$$

The obtained simulation results of the FO position coordinate errors ΔX, ΔY, ΔZ, the FO flight trajectory and the position error FO were plotted graphically in Figs. 2 and 3. Fig. 2 shows a selected section of the FO flight trajectory between 200 and 220 seconds of flight.

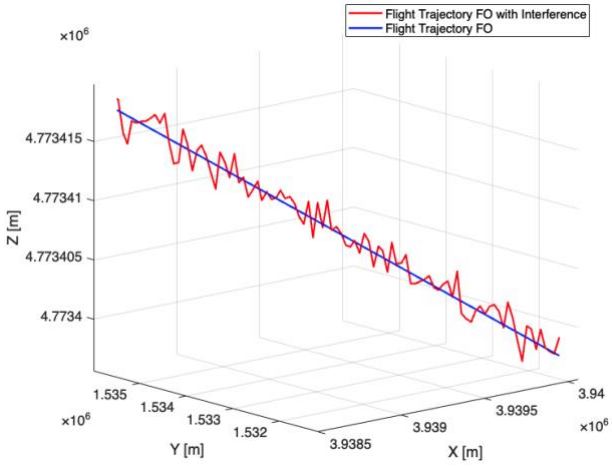

FIGURE 2. FO trajectory segment after accounting for errors for *k* = 1.

Two FO flight trajectories are shown in the graph. The original flight trajectory, shown in blue, represents the FO flight path without errors when determining its position. The FO flight trajectory, which is determined by the X, Y and Z coordinates, is shown in red and considers the errors in the measurement of the FO coordinates by the satellite navigation system. This flight trajectory will henceforth be referred to as the measured FO flight trajectory. The measured trajectory follows the basic trend of the original trajectory, showing visible deviations from the original FO flight trajectory due to inaccurate measurements. These deviations are manifested as changes in all three X, Y and Z coordinates relative to the coordinates of the original modelled FO flight trajectory without errors. The progression of the errors ΔX,ΔY,ΔZ, and ΔP is shown in Fig. 3.

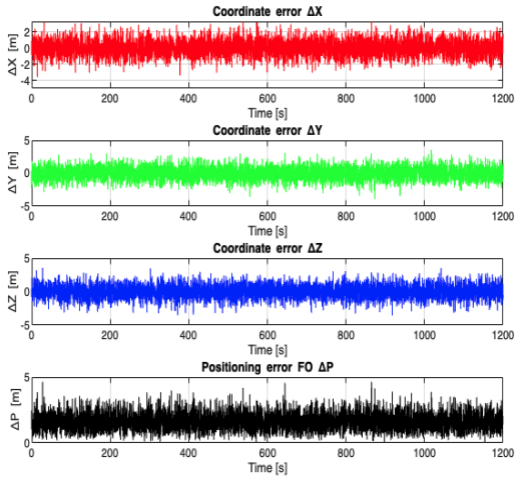

FIGURE 3. Time dependence of the errors of the coordinates ΔX, ΔY, ΔZ, and the position of the FO ΔP.

The dependence of the errorΔ X on time is shown in red. This error varies from -5m to + 5m. The mean value of error (MVE) $\mu\Delta X$ was equal to 0.00548 m, and the mean square error (MSE) $\sigma^2_{\Delta X}$ was equal to 0.98149 m^2. The dependence of the ΔY error on time is shown in green. This error varies from -5 m to + 5 m meters, MVE $\mu_{\Delta Y}$ was equal to 0.00332 m, and the MSE $\sigma^2_{\Delta Y}$ was equal to 1.00929 m^2 . The dependence of the ΔZ error on time is shown in blue. This error varies from -5 m to + 5 m, MVE $\mu_{\Delta Z}$ was equal to -0.01588 m, and the MSE $\sigma^2_{\Delta Z}$ was equal to 1.04121 m^2. The dependence of the position measurement errorΔP on time is shown in black. This error varies from 0.0 m to + 5 m meters, MVE $\mu_{\Delta P}$ was equal to 1.58711 m, and MSE $\sigma^2_{\Delta P}$ was equal to 0.44147 m^2.

The histogram of the error distribution of the ΔX,ΔY,ΔZ coordinates, and the FO position ΔP is shown in Fig. 4.

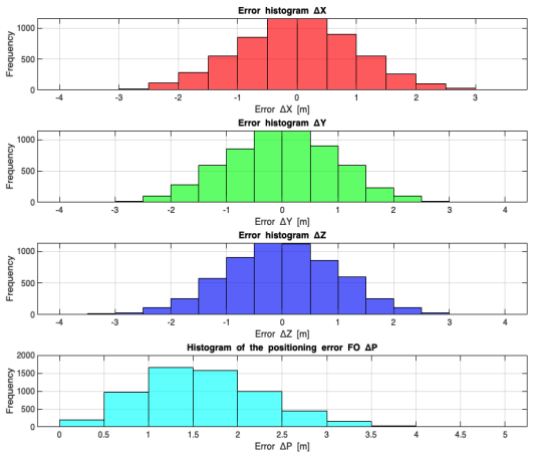

FIGURE 4. Time Histogram of the distribution of errors of ΔX, ΔY, ΔZ coordinates, and FO position PΔ

In the simulation, the constant k, which can vary the magnitude of the errors of the individual coordinates according to relations (7 to 9), was equal to one. From the figure, the coordinate errors of the FO trajectory are

distributed according to a normal law with the above parameters.

Based on the developed models, we obtained the error-free FO positioning flight trajectory and the so-called measured FO flight trajectory, which considers the measurement errors of the receiver of the satellite navigation system user by simulation. In our research, we sought to filter out FO position measurement errors as much as possible. The magnitude of these errors was varied using a constant k according to relations (7 to 9).

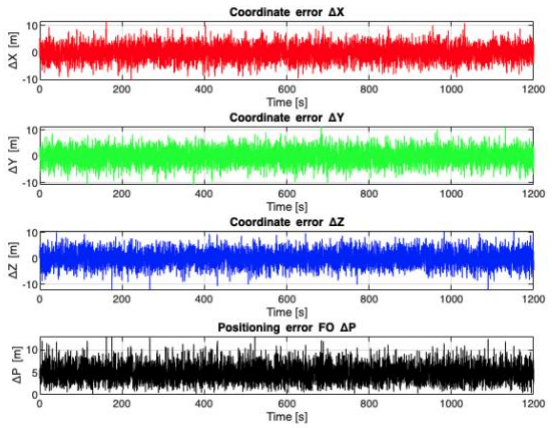

FIGURE 5. Dependence of the errors of the coordinates ΔX, ΔY, ΔZ and the position FO ΔP on time for the constant *k=3*.

Figure 5 shows the dependence of the errors ΔX, ΔY, ΔZ and ΔP on time for k=3. The error ΔX, shown in red, varies from -10 m to +10 m with MVE μΔX of 8.86284 m, and a MSE $\sigma^2_{\Delta X}$ =8.8624 m². The error ΔY, shown in green, varies between -10 m and +10 m, with a MVE μΔY of 8.94696 m, and a MSE $\sigma^2_{\Delta Y}$ = 8.94695 m². The blue curve represents the error ΔZ, which varies in the same interval with MVE μΔZ = 8.91795 m, and a MSE $\sigma^2_{\Delta Z}$ = of 8.9165 m². Finally, the positioning error ΔP, shown in black, varies from 0 m to +10 m, MVE μΔP was 26.72775 m, and MSE $\sigma^2_{\Delta P}$ of 4.0867 m². The coordinate errors ΔX, ΔY, ΔZ, and ΔP for k=5 are shown in Fig. 6.

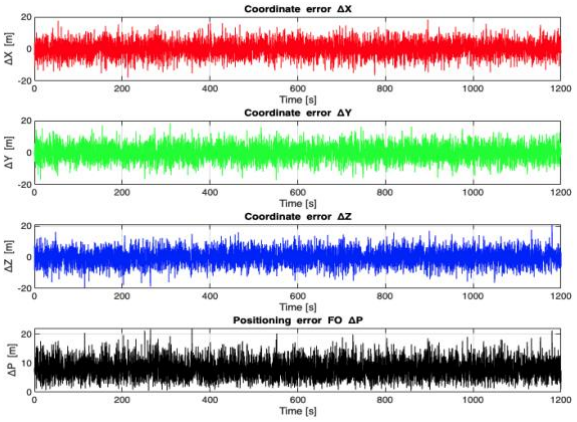

FIGURE 6. Dependence of the errors of the coordinates ΔX, ΔY, ΔZ and the position FO ΔP on time for the constant *k=5*

The ΔX error varies from -20 m to +20 m. MVE μΔX is equal to 24.47239 m, and the MSE $\sigma^2_{\Delta X}$ is equal to 24.45943 m². The ΔY error in a similar range, MVE μΔY equal to 24.56159 m, and the MSE $\sigma^2_{\Delta Y}$ equal to 24.5577 m². The blue curve, representing the ΔZ error, shows similar variances with MVE μΔZ values of 24.47398 m, and MSE $\sigma^2_{\Delta Z}$ = 24.47078 m² . The black curve shows the error ΔP, which varies from 0 m to +20 m. The MVE μΔP is equal to 73.50796 m, and the MSE $\sigma^2_{\Delta P}$ is equal to 11.17707 m². The simulation results confirm that the magnitude of the FO trajectory measurement errors can be varied using the constant.

The means and variances of these errors for a constant k equal to 1 to 5 are shown in Figs. 7 and 8.

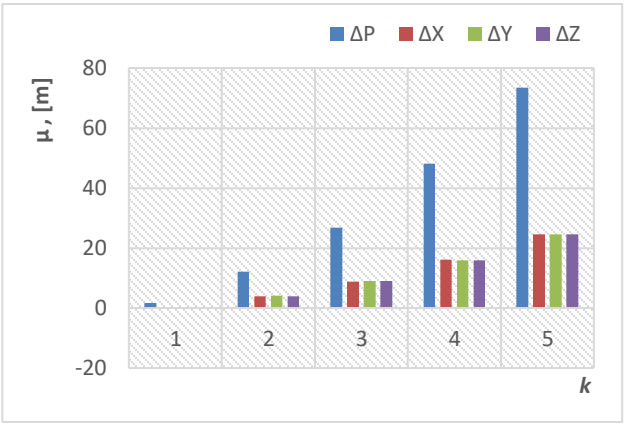

FIGURE 7. Mean errors of ΔX, ΔY, ΔZ coordinates and FO ΔP position as a function of the constant *k*

The mean values of the $\mu_{\Delta X,Y,Z}$ coordinate errors ΔX, ΔY, ΔZ, and FO position error ΔP versus the constant k demonstrate the direct correlation between the coordinate error and the position error. From the results, as the coordinate error ΔX, ΔY, ΔZ increases, there is a significant increase in the total position error ΔP. This dependence indicates that the accuracy of the FO coordinate measurement fundamentally affects its positioning accuracy. In the simulations, the mean coordinate errors varied from -0.015 m to 73.5 m.

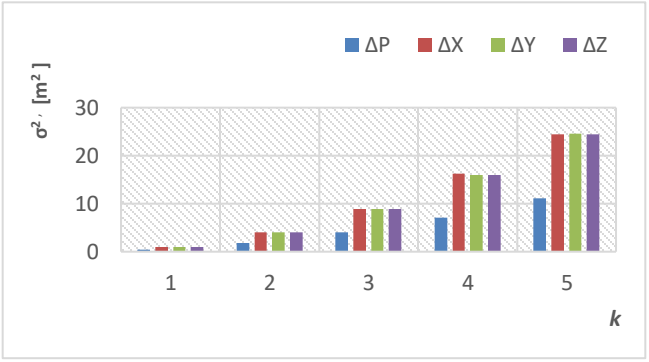

FIGURE 8. Mean square error of ΔX, ΔY, ΔZ coordinates and FO ΔP position as a function of the constant *k*

The subject of further research was the search for methods to reduce errors in measuring the FO flight trajectory. We investigated the use of linear and nonlinear filters and the application of neural networks in processing FO attitude data. One possibility was using the Savitzky-Golay filter to smooth the signals without losing their main shape. This filter applied a polynomial approximation within a moving window for each point in the flight trajectory, thus reducing the measurement errors of the flight trajectory while preserving its original shape. A feedforward neural network was also implemented to correct the FO flight trajectory by comparing the original and error data. The network was trained using the Levenberg-Marquardt algorithm, allowing fast and efficient adjustment of the network weights. The network's performance was optimized over 3000 epochs, where the network minimized the errors between the original and erroneous coordinate values. Our solution is based on combining the Savitzky-Golay filter with an advanced neural network to achieve the most accurate measurement of the actual FO flight trajectory.

IV. Application of Savitzky – Golay filter for GNSS signal processing

Using the Savitzky-Golay filter in GNSS signal processing is appropriate due to the need to measure the FO flight trajectory, which should not be degraded by interference. This filter reduces measurement errors well and does not significantly affect the nature of the flight trajectory. It is particularly suitable for filtering out white noise processes that cause fluctuations in the FO position measured by the GNSS receiver. We used the Savitzky-Golay filter to remove errors in the FO flight trajectory measurements. It is a digital filter designed for data smoothing. This filter is specifically designed to minimize high-frequency noise. It works on the principle of polynomial approximation of the data in each window (so-called "sliding window"). In each window, a polynomial of a certain degree is filtered (in our case, it is a third-degree polynomial), and the result is computed by using this polynomial to approximate the central value in the window. The Savitzky-Golay filter is defined as the minimization of the sum of squares of the outliers for a chosen window of data. The filter looks for the polynomial that best represents the values in the window and then computes the value at the central position. Its formulation is advantageous because, while preserving the signal's shape, it removes mostly random noise and does not affect the trend of the signal. This approach is often beneficial when processing data from GNSS receivers, where it is essential to remove the effect of noise while measuring the exact flight trajectory [30]. This filtering technique uses a window of size w, 51 points, and a polynomial degree p, where p=3. For each point in the signal, we compute a value by fitting a third-degree polynomial to the surrounding 51 points. We repeat this process for each point in the signal. Determined parameters affect the filter's ability to capture the signal's trend. A larger window smoothes the signal more, while a minor polynomial degree preserves only the underlying signal trends for polynomial fitting using the least squares method [30].

For each point i in the sliding window, the estimated value of the signal y_i is computed using a polynomial of degree p of the form:

$$y_i = \sum_{j=0}^{p} c_j x_i^j \tag{14}$$

where
y_i is approximated signal value at point,
x_i is input value (distance from the center of the window),
c_j are coefficients of a polynomial of order p.

The coefficients cj are calculated using the least squares method, which minimizes the sum of squares of the differences between the actual noisy values and the values predicted by the polynomial within the window. For the vector of coefficients, holds [29]:

$$c = (X^T X)^{-1} X^T y \tag{15}$$

where:
X is a matrix of input values in which each row corresponds to the powers of the points in the window $(1,x,x^2,...,x^p)$,
y is the vector of noise values in the sliding window,
c is a vector of coefficients $(c_0,c_1,...,c_p)^{(T)}$.

For the inverse $(X^T X)^{-1}$ to exist, the matrix X must have full column rank, meaning that its columns must be linearly independent. In the context of the sliding window, this implies that the points within the window must be sufficiently diverse to uniquely determine the polynomial coefficients.

The Savitzky-Golay filter is implemented in Matlab. The MATLAB function sgolayfilt was used for the Savitzky-Golay filter in this study. However, this filter is also available in open-source software, for example in Python (scipy.signal.savgol_filter) or can be implemented using standard polynomial least-squares smoothing methods. The Savitzky-Golay filter is a convolutional filter, where the coefficients q_j are predefined for each point in the window. These coefficients are computed based on the least squares method and allow the filtering of the values for each point without the need for repeated regression. Once the coefficients are calculated for a particular window, the filtered value for the centre point of the window is given as a linear combination of the values of the points in the window. This linear combination is:

$$\hat{y}_i = \sum_{j=-n}^{n} q_j . y_i + j \tag{16}$$

where qj are filter-specific convolution coefficients and are computed directly from the polynomial fit in a window of size w=2n+1.
For each value of the coordinate $X_{filtered}[i]$:

$$X_{filtered}[i] = \sum_{j=-n}^{n} q_j . X_{er}[i+j] \tag{17}$$

Where:
$X_{er}[i]$ is the value of the noise signal for point i,
$X_{filtered}[i]$ is the filtered signal value for point i.
The same calculations are performed for the Y and Z coordinates.

The values for the individual coordinates $X_{filtered}$, $Y_{filtered}$ and $Z_{filtered}$ are calculated in Matlab using the sgolayfilt function as follows:

$$X_{filtered} = \text{sgolayfilt}(X_{er}, 3, 51) \quad (18)$$
$$Y_{filtered} = \text{sgolayfilt}(Y_{er}, 3, 51) \quad (19)$$
$$Z_{filtered} = \text{sgolayfilt}(Z_{er}, 3, 51) \quad (20)$$

We express the coordinate errors at the filter output as the difference between the coordinate values at the filter output and the coordinates of the flight trajectory without errors:

$$\Delta X_{filtered} = X_{filtered} - X_{true} \quad (21)$$
$$\Delta Y_{filtered} = Y_{filtered} - Y_{true} \quad (22)$$
$$\Delta Z_{filtered} = Z_{filtered} - Z_{true} \quad (23)$$

The FO positioning error ΔP_{filt} is equal to:

$$\Delta P_{filt} = (\Delta X_{filt}^2 + \Delta Y_{filt}^2 + \Delta Z_{filt}^2)^{0.5} \quad (24)$$

The flight trajectory simulation results from the output of the Svitzky-Golay filter are shown in Figs. 9 and 10.

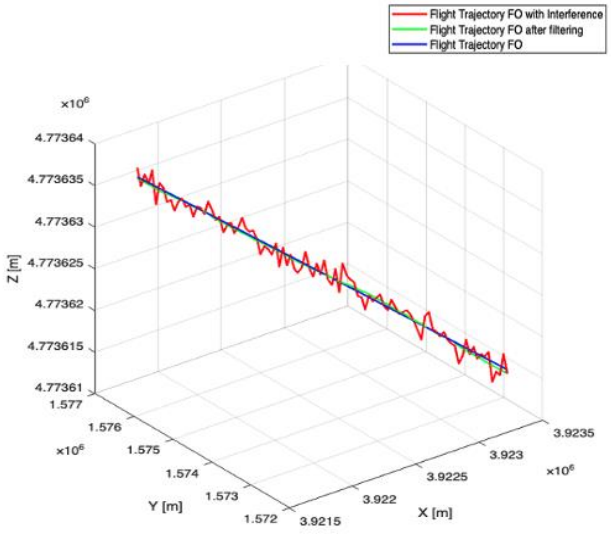

FIGURE 9. A section of the FO flight trajectory determined without errors and from the output of the Savitzky-Golay filter for *k* = 1.

The trajectory of the calculated FO flight trajectory after applying the Savitzky-Golay filter, which is shown in green, is like the trajectory of the FO flight trajectory without errors, which is shown in blue. The computed FO flight trajectory follows the basic trend of the original FO flight trajectory and does not show significant deviations from the original FO flight trajectory. This confirms that the Savitzky-Golay filter has removed the fluctuations in the flight trajectory caused by the measurement inaccuracy. Therefore, this filter is suitable for applications in air navigation.

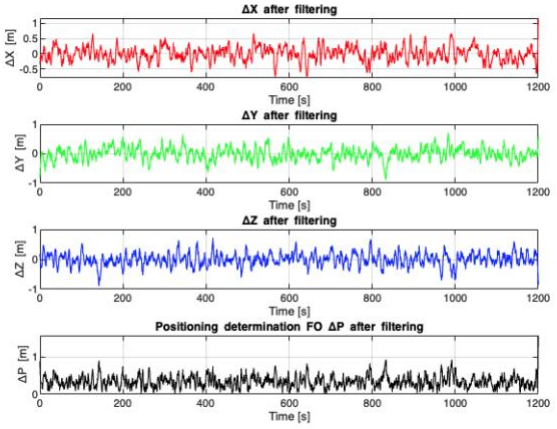

FIGURE 10. Dependence of coordinate errors ΔX, ΔX, ΔZ, and FO position ΔP from the output of the Savitzky-Golay filter.

In Fig. 10, the dependence of the error ΔX on time is shown in red. This error varies from 0 m to +1 meter. MVE μΔX was equal to 0.00545 m, and MSE $\sigma^2_{\Delta X}$ was equal to 0.03519 m^2. The dependence of the ΔY error on time is shown in green. This error varies from -1 m to +1 m. MVE μΔY error was equal to 0.00320 m, and MSE $\sigma^2_{\Delta Y}$ was equal to 0.04414 m^2. The dependence of ΔZ error on time is shown in blue. This error varies from -1 m to +1 m. MVE μΔZ was equal to -0.01606 m, and MSE $\sigma^2_{\Delta Z}$ was equal to 0.04337 m^2. The dependence of the position measurement errorΔP on time is shown in black. This error varies from 0.0 m to + 0.8 m. MVE μΔP was equal to 0.32160 m, and MSE $\sigma^2_{\Delta P}$ was equal to 0.01957 m^2.

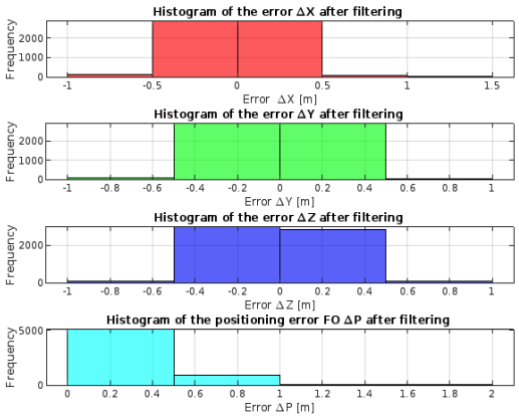

FIGURE 11. After filtering, the histogram of the error distribution of ΔX, ΔY and ΔZ coordinates and FO ΔP position

The error filtering histogram of the ΔX,ΔY,ΔZ coordinates and the FO position ΔP, which is shown in Fig. 11, shows that the filter suppressed the fluctuations of the FO flight trajectory and changed the distribution of the errors to uniform. It is clear from the histogram that the errors of the coordinates ΔX,ΔY,ΔZ are in the range of -1m to +1m. For example, most of the errors of the X coordinate are in the range of -0.5m to +0.5 m. The errors of determining the position FO ΔP are positive in accordance with equation 13 and vary in the range from 0m to 1m.

Further research verified how the Savitzky-Golay filter would respond to more significant errors in the flight trajectory measurement. We simulated the errors in the flight trajectory measurement using equations (7 to 9). The statistics for these errors are shown in Figure 8 and Figure 9. The results of filtering the flight trajectory signals using the Savitzky-Golay filter for a k equal to 1 to 5 are shown in Fig. 14 and Fig. 15

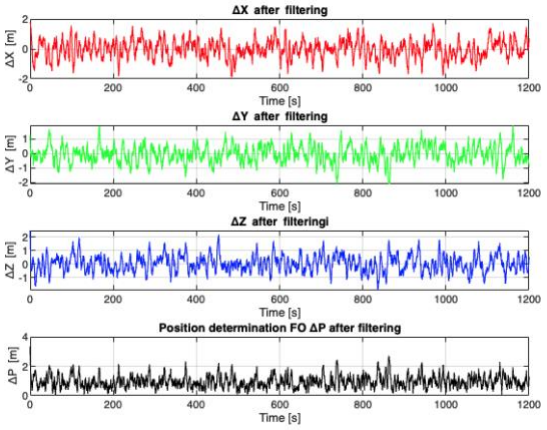

FIGURE 12. Dependence of the coordinate errors ΔX, ΔX, ΔZ and FO position ΔP on time after applying the Savitzky-Golay filter for costant k=3.

After applying the Savitzky-Golay filter for k=3, the dependence of individual errors on time was analyzed. Figure 12 shows the dependence of the error ΔX on time in red. The values of this error vary in the interval from -4 m to +4 m, with ME μΔX equal to 0.36542 m, and MSE $\sigma^2_{\Delta X}$= 0.37335m². The error ΔY is shown in green and its values vary between -5 m and +5 m. MVE μΔY is 0.36927 m, and MSE $\sigma^2_{\Delta Y}$ is equal to 0.36925 m². The blue colour represents the ΔZ error, which varies between -4 m and +2 m. MVE μΔZ of this error was equal to 0.3738 m, and MSE $\sigma^2_{\Delta Z}$ was equal to 0.36396 m². The FO positioning error ΔP varied from 0 to +6 m.

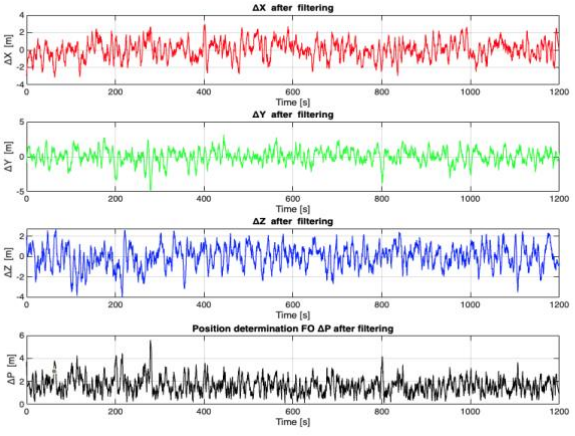

FIGURE 13. Dependence of the coordinate errors ΔX, ΔX, ΔZ and FO position ΔP on time after applying the Savitzky-Golay filter for constant k=5.

Figure 13 shows the error traces ΔX, ΔY, ΔZ and ΔP after applying the Savitzky-Golay filter for the constant k=5. The error ΔX varies from -4 m to +4 m, with MVE μΔX being 1.09894 m, and the MSE $\sigma^2_{\Delta X}$ being equal to 1.08595 m². The error ΔY varies from -5 m to +5 m, with a MVE μΔY equal to 1.10712 m, and a MSE $\sigma^2_{\Delta Y}$ equal to 1.10309 m². The error ΔZ follows a similar pattern, with values ranging from -4 m to +2 m, with a MVE μΔZ equal to 1.05103 m, and a MSE $\sigma^2_{\Delta Z}$ equal to 1.04775 m². The FO positioning error ΔP varies from 0 m to +6 m. MVE μΔP is equal to 3.25708 m, and MSE $\sigma^2_{\Delta P}$ is equal to 0.52522 m². The simulation showed that the application of the Savitzky-Golay filter contributed to a significant reduction of the FO flight trajectory measurement errors, while preserving the true FO flight trajectory.

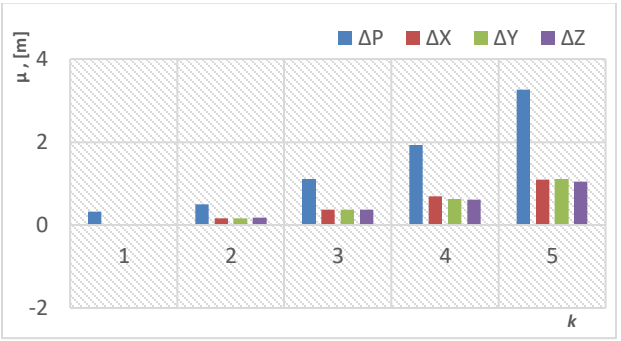

FIGURE 14. Mean value of errors of coordinates ΔXfilt, ΔYfilt, ΔZfilt and FO position ΔPfilt after filtering with the Svitzky-Golay filter for k = 1 to 5.

Mean value of errors μΔX,Y,Z of coordinates ΔXfilt, Yfilt, ΔZfilt, and FO position ΔPfilt after filtering with the Savitzky-Golay filter for k = 1 to 5 were equal from 0.01 m to 3.25 m.

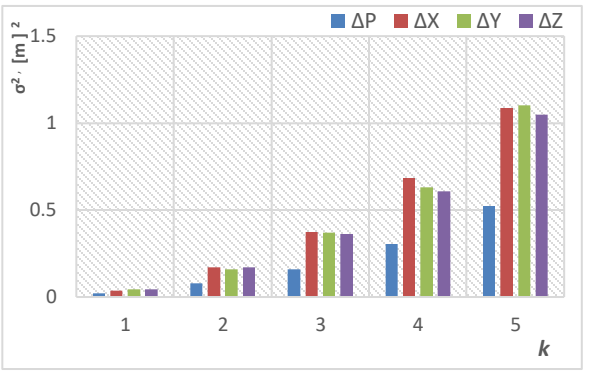

FIGURE 15. Mean square errors of coordinates ΔXfilt, ΔYfilt, ΔZfilt and FO position ΔPfilt after filtering with the Svitzky-Golay filter for k = 1 to 5.

Mean square errors $\sigma^2_{\Delta X,Y,Z}$ of the coordinates ΔXfilt, ΔXfilt, ΔZfilt and the positions of FO ΔPfilt after filtering with the Savitzky-Golay filter for k = 1 to 5 were equal to 0.01 m^2 to 1.1 m^2.

The simulation results confirmed that the proposed Savitzky-Golay filter significantly reduced the measurement errors of X, Y, and Z coordinates and FO positions. After filtering, all the FO flight trajectory parameters deviate less

from the accurately determined FO flight trajectory than the FO flight trajectory coordinates under inaccurate FO position measurement.

V. Neural network design for gnss signal processing

In some GNSS applications, exact FO position measurement is required. Therefore, a neural network design was performed to provide error correction for inaccurate FO flight trajectory measurements. In our case, we designed a feedforward neural network which has:

- Input layer with three neurons corresponding to the filtered coordinates (Xfiltered,Yfiltered,Zfiltered)
- Two hidden layers with 40 and 20 neurons, where each neuron has weights that we optimize during training,
- Output layer with three neurons corresponding to the corrected coordinates (Xcorrected, Ycorrected, Zcorrected)

We express the output of each neuron in the hidden layer by the relation:

$$y_j^{(m)} = \frac{1}{1+e^{-(\sum_i w_{ji}^{(m)} \cdot h_i^{m-1} + b_j^{(m)})}} \quad (25)$$

Where:

h_i^{m-1} is the output of the neuron for i in the previous layer (m - 1),

$w_{ji}^{(m)}$ is the weight connecting neuron i in layer (m-1) to neuron j in layer l,

$b_j^{(m)}$ is the bias of neuron j in layer l,

The network was trained using weights and biases to minimize errors between predicted values ($\hat{X}, \hat{Y}, \hat{Z}$) and target values (X,Y,Z). We express the errors in terms of the mean square errors (MSE) using the formula:

$$MSE = \frac{1}{N}\sum_{n=1}^{N}((x_n - \hat{X}_n)^2 + (Y_n - \hat{Y}_n)^2 + (Z_n - \hat{Z}_n)^2 \quad (26)$$

where N is the number of trained instances.

The Levenberg - Marquard algorithm, which combines the properties of Gauss - Newton and gradient descent methods, was used in the neural network. Updating with error gradients and the Hessian matrix allows us to converge quickly to the minimum error value. We approximate the Hessian matrix H as [30]:

$$H \approx J^T J , \quad (27)$$

where J is the Jacobian matrix of the derivatives of the errors under the weights.

The weights are updated according to the relationship:

$$w^{(k+1)} = w^{(k)} - (J^T J + \lambda . \mathrm{diag}(J^T J))^{-1} J^T e \quad (28)$$

Where:

λ is the damping parameter that controls the transition between gradient descent and the Gauss- Newton method,

I is the unit matrix,

e is the error vector.

After training the network on the filtered input data, the coordinate correction is applied as follows:

$$\begin{bmatrix} \hat{X}_{corrected} \\ \hat{Y}_{corrected} \\ \hat{Z}_{corrected} \end{bmatrix} = \mathrm{net}\left[\begin{pmatrix} X_{corrected} \\ Y_{corrected} \\ Z_{corrected} \end{pmatrix}\right] \quad (29)$$

From the output of the neural network, we obtain coordinates that correspond to the actual flight trajectory of the FO, while minimizing the measurement errors.

The measurement error of the X, Y and Z coordinates is determined as follows:

$$\Delta X_c = \hat{X}_c - X, \quad (30)$$

$$\Delta Y_c = \hat{Y}_c - Y, \quad (31)$$

$$\Delta Z_c = \hat{Z}_c - Z, \quad (32)$$

We determined the FO ΔP positioning error by Eq:

$$\Delta P = (\Delta X^2 + \Delta Y^2 + \Delta Z^2)^{0.5} \quad (33)$$

The neural network model (Figure 16) was designed to improve the accuracy of the FO position measurement in case of errors in its position measurement. The data obtained by erroneous FO position measurement was fed to the input of the Savitzky-Golay filter and then corrected from its output by the proposed neural network to minimize the FO coordinate measurement errors.

The neural network was designed with three layers: an input layer, two hidden layers, and an output layer. Each neuron in the hidden layer is connected to all neurons in the next layer. These neurons work by applying weights to the inputs and combining them with biases, passing through an activation function. The output layer has three neurons that provide the corrected X, Y and Z coordinate values.

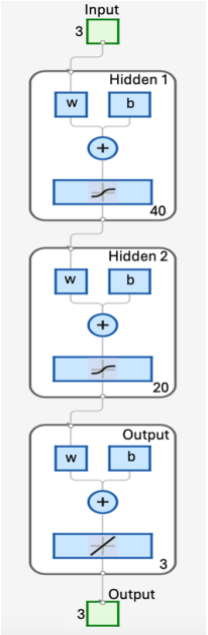

FIGURE 16. Neural network model

The Levenberg-Marquardt algorithm was used to train the neural network. This algorithm is a kind of gradient descent and is very efficient for processing signals with small to medium interference intensity. It has the speed and reliability advantage and is, therefore, very suitable for correcting real-time data such as flight trajectories [30]. Although the Savitzky-Golay filter has lower computational complexity compared to the Kalman filter, combining this filter with a neural network can introduce additional computational overhead. However, in our implementation, neural network training is performed offline (elapsed time: 12 minutes and 52 seconds, tab. 1), while real-time application only involves a single feedforward computation, which is generally faster than the iterative Kalman filter. Therefore, the proposed solution is practically feasible for real-time signal processing. The training was run for 3000 epochs, meaning that the model iterated through the training dataset 3000 times to optimize the weights and reduce the error between the predicted and actual coordinate values. To avoid overfitting, we randomly split the dataset into 70 percent for training and 30 percent for testing. The training set included data from the output of the Savitzky - Golay filter and the reference coordinates of the FO flight trajectory. The neural network was trained exclusively on the training data, and its performance was evaluated on the separate test set. The neural network was trained exclusively on the training set, and its performance was evaluated on the independent test set. The proposed neural network can reconstruct the original FO flight trajectory based on inaccurate data.

TABLE I
NEURAL NETWORK TRAINING

Unit	Initial value	Stopped value	Target value
Epoch	0	3000	3000
Elapsed time	-	0:12:52	-
Performance	2.64^{e+10}	0.00861	0
Gradient	1.44^{e+11}	961	$1e^{-07}$
MU	0.001	0.01	1^{e+10}
Validation checks	0	0	6

During training, the neural network's performance improved steadily, which is also visible in the training results, where the error decreased significantly. The resulting gradient values, which reached a level of 961, show the successful convergence of the model, which is crucial for a good prediction. The overall performance of the network reached 0.00861, which is a very low FO coordinate error value. The FO flight trajectory measurement simulation results using the Savitzky-Golay filter and the neural network are shown in Figs. 17 and 18.

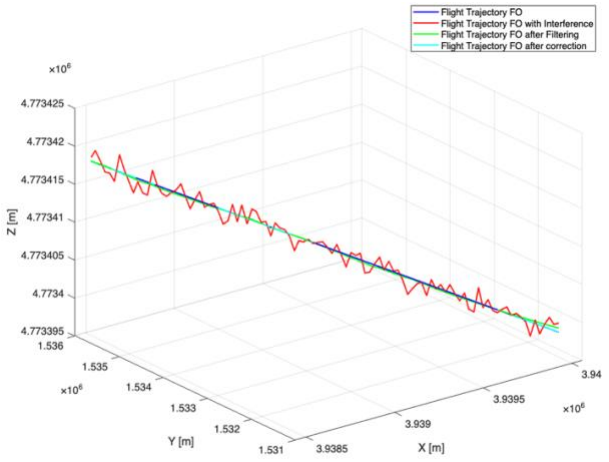

FIGURE 17. Section of the FO flight trajectory from the Savitzky-Golay filter and neural network output

The trajectory of the simulated FO flight trajectory from the output of the Savitzky-Golay filter and the neural network, which is shown in green, is almost identical to the trajectory of the FO flight trajectory without errors, which is shown in blue. The simulated FO flight trajectory follows the basic trend of the original FO flight trajectory and shows very small deviations from the original FO flight trajectory. This confirms that the use of a combination of Savitzky-Golay filter and neural network in GNSS signal processing effectively removes the flight trajectory fluctuations caused by measurement inaccuracy. Therefore, such a method of processing GNSS data that are degraded by interference is suitable for applications in the field of aeronautical navigation.

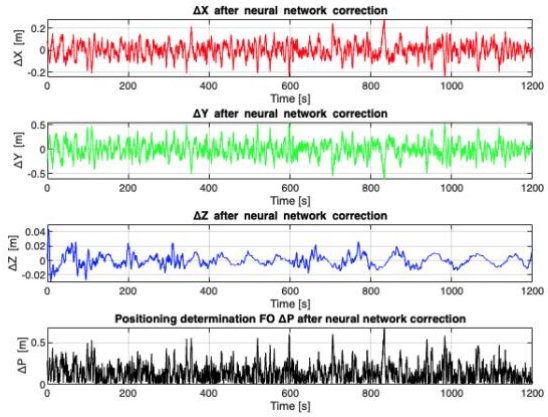

FIGURE 18. Section Time dependence of coordinate errors ΔX, Δ, ΔZ and FO position ΔP from the neural network output.

Fig. 18 shows the dependence of the error ΔX on time in red. This error varies from -0.2 m to + 0.2 m. MVE μΔX was equal to 0.00137 m, and the MSE $\sigma^2_{\Delta X}$ was equal to 0.00385 m^2. The dependence of the ΔY error on time is shown in green. This error varies from -0.5 m to + 0.5 m. MVE μΔY was equal to -0.00457 m, and MSE $\sigma^2_{\Delta Y}$ was equal to 0.02060 m^2 . The dependence of the ΔZ error on time is shown in blue. This error varies from -0.02 m to + 0.04 m. MVE μΔZ was equal to 0.00007 m, and MSE $\sigma^2_{\Delta Z}$ was equal to 0.00004

m². The dependence of the FO ΔP position measurement error on time is shown in black. This error varies from 0.0 m to + 0.5 m. MVE μΔP was equal to 0.12457 m, and MSE $\sigma^2_{\Delta P}$ was equal to 0.00899 m².

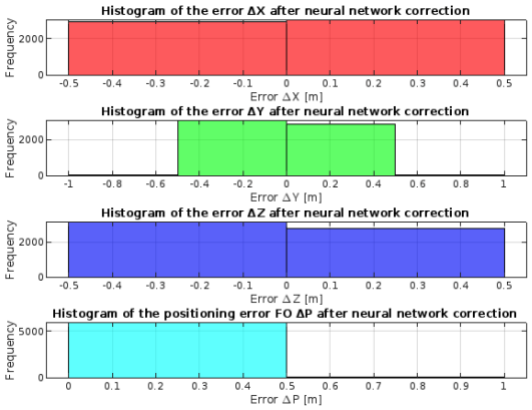

FIGURE 19. Error distribution histogram of ΔX, ΔY, ΔZ, and FO ΔP coordinate positions from the neural network output.

From the error histogram of the ΔX, ΔY, ΔZ coordinates and the FO ΔP position, the neural network suppressed the fluctuations of the FO flight trajectory and did not change the density of the error probability distribution. It is clear from the histogram that the errors of the ΔX, and ΔZ, coordinates range from -0.5 m to 0.5 m and the error of ΔY coordinate varies in the range from -1 m to +1. The errors of determining the position of the FO ΔP are positive in accordance with equation 13 and vary in the range from 0 m to 1 m. The simulation results confirmed that the proposed Savitzky-Golay filter and neural network significantly reduced the measurement errors of X, Y, and Z coordinates and FO positions. After filtering, all the FO flight trajectory parameters have much more minor deviations from the accurately determined FO flight trajectory than the FO flight trajectory coordinates under inaccurate FO position measurement. The application of a neural network in processing the data from the user's GNSS receiver output allows the achievement of very high accuracy of the FO position measurement, which is crucial for the safety and reliability of navigation in aviation.

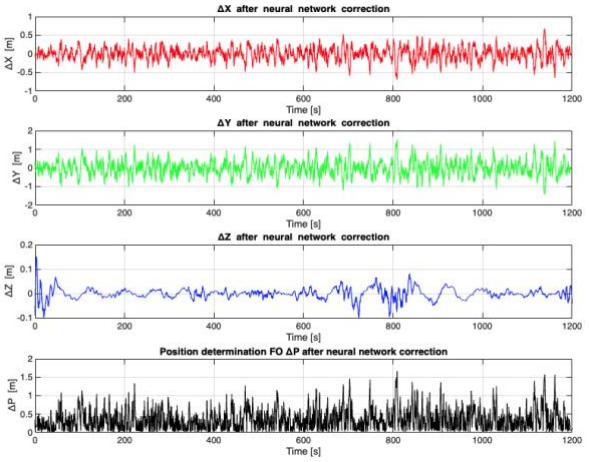

FIGURE 20. Time dependence of coordinate errors ΔX, Δ, ΔZ and FO position ΔP from the neural network output for the constant k=3

Figure 20 shows the error traces of ΔX, ΔY, ΔZ, and ΔP after neural network correction for *k=3*. The error of ΔX ranges from -1 m to +1 m, while MVE $\mu_{\Delta X}$ was equal to 0.03862 m, and MSE $\sigma^2_{\Delta X}$ reaches the exact value of 0.03862 m². The error ΔY varies from -2 m to +2 m with a MVE $\mu_{\Delta Y}$ of 0.20554 m and a MSE $\sigma^2_{\Delta Y}$ of 0.20552 m². The error ΔZ has a range from -01 m to +0.2 m, with MVE $\mu_{\Delta Z}$ and MSE $\sigma^2_{\Delta Z}$ of the same value 0.00015 m. The positioning error ΔP varies from 0 m to +2 m, MVE $\mu_{\Delta P}$ of 0.24431 m, and MSE $\sigma^2_{\Delta P}$ of 0.08833 m².

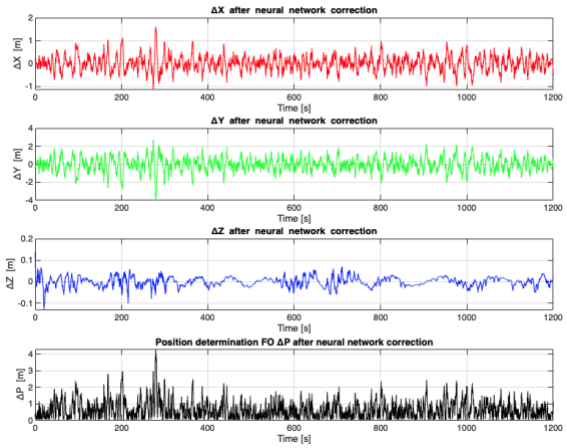

FIGURE 21. Time dependence of coordinate errors ΔX, Δ, ΔZ and FO position ΔP from the neural network output for the constant k=5

The error plot of ΔX, ΔY, ΔZ and ΔP after applying the neural network correction also for *k*=5 shows an improvement in the accuracy of the FO flight trajectory measurement (Figure 21). The ΔX error varies from -1 m to +2 m, MVE $\mu_{\Delta X}$ is 0.09417 m, and MSE $\sigma^2_{\Delta X}$ is 0.09416 m². The error ΔY varies from -4 m to +4 m, with MVE $\mu_{\Delta Y}$ of 0.49877 m and MSE $\sigma^2_{\Delta Y}$ of 0.4987 m². The ΔZ error shows the lowest variation from -0.1 m to +0.2 m, with MVE $\mu_{\Delta Z}$ of 0.00085 m and MSE $\sigma^2_{\Delta Z}$ of 0.00085 m². The positioning error ΔP ranges from 0 m to +4 m, with MVE $\mu_{\Delta P}$ of 0.5938

m and MSE $\sigma^2_{\Delta P}$ of 0.22081 m². These results show that the neural network reduces the FO flight trajectory measurement errors in all observed parameters.

VI. Discussion

This paper focused on applying neural networks and the Savitzky-Golay filter to correct FO flight trajectories measured by GNSS with errors. The main objective was to remove the errors in the FO flight trajectory measurements and determine to what extent the positional data FO could be obtained after applying the filter and by using neural network correction. The applied Savitzky-Golay filter followed the FO trajectory without losing its original shape significantly. This had the effect of reducing the scatter and increasing the accuracy of the FO position data, but the filter did not completely remove the errors in the FO flight trajectory measurements.

The application of the neural network, which was trained with the Levenberg-Marquardt algorithm, represented a step towards a higher level of correction accuracy. The neural network learned the relationships between the erroneous and original data. It effectively minimised the FO positioning errors, and the resulting mean error and variance values after network application were very low. The three-layer network provided sufficient performance to capture and correct the FO position measurement errors, while the Levenberg-Marquardt algorithm provided effective training even with many epochs. Although the results were very accurate, the application of neural networks in aviation requires further testing under different disturbance conditions and with an increase in the robustness of the model to unexpected deviations.

Compared to other works, our approach has yielded similar or even better results in data processing under GNSS interference conditions. For example, in [18], a low-cost GNSS interference monitoring system was proposed, utilising digital signal processing methods. The authors present the results of testing their system, achieving an interference detection accuracy of 95%. In the study [19], machine learning techniques were used for GNSS interference monitoring and machine learning was shown to give very good results in interference detection and classification, but an application to FO trajectory correction was not part of the work. In terms of localization, they achieved a mean absolute error (MAE) of less than 2.5 meters, indicating the system's high accuracy in locating interference sources.

On the contrary, the works [20, 21] show the potential of neural networks in GNSS interference detection and classification. In [21], the ability of the network to detect a wide range of interference with high accuracy was demonstrated, suggesting that similar techniques could be effective in trajectory error correction. Their approach achieved a high interference classification accuracy of 99.69%, even at low interference signal levels. Our research contributes to using a combination of the Savitzky-Golay filter and neural network correction of GNSS signals, which can achieve better FO positioning accuracy.

Compared to the work of [24], where digital filters were used to process GNSS data in railway applications, our approach adds a layer of accuracy using machine learning, allowing unexpected outliers to be better handled. The authors report that they achieved track positioning accuracy of approximately 0.5 m using the proposed system and methods. Also, the results presented in [25], where the response of digital filters was analysed, confirm that filtering alone is often insufficient to remove the interference, which corresponds to our findings completely.

This study shows that the combination of Savitzky-Golay filters and neural networks is an effective tool for GNSS signal processing and has the potential for aeronautical applications where the accuracy and reliability of FO position data are critical for navigation safety and efficiency. Our method provides not only interference minimization but also high-accuracy reconstruction of original trajectories.

VII. Conclusion

The results of this study confirm that combining classical filtering methods with advanced neural networks can yield significant improvements in the accuracy of recovering FO positional data corrupted by interferences. The FO flight trajectory model, developed based on realistic parameters, included initial coordinates over Košice Airport and simulated a left-handed curvilinear path at a constant speed of 222.22 m/s and an altitude of 10,000 meters. Randomly generated errors were added to the FO flight trajectory model to simulate GNSS system interference.

The Savitzky-Golay filter reduced trajectory measurement errors while preserving the trajectory shape. After applying the filter, MVE $\mu_{\Delta X}$ for the X coordinate was reduced to 0.00545 m, and MSE $\sigma^2_{\Delta X}$ was reduced to 0.03519 m². For the Y coordinate, MVE $\mu_{\Delta Y}$ was equal to 0.00320 m and MSE $\sigma^2_{\Delta Y}$ was equal to 0.04414 m². For the Z coordinate, MVE $\mu_{\Delta Z}$ was equal to -0.01606 m, and the MSE $\sigma^2_{\Delta Z}$ was equal to 0.04337 m². The overall FO positioning error decreased after filtering. The MVE $\mu_{\Delta P}$ was equal to 0.32160 m, and the MSE $\sigma^2_{\Delta P}$ was equal to 0.01957 m². These results confirm that the filter partially removed the FO flight trajectory measurement errors but could not eliminate all the interference effects.

Adding a neural network to the Savitzky-Golay filter resulted in an even more significant improvement in the accuracy of the FO flight trajectory measurement. The proposed three-layer network was trained using the Levenberg-Marquardt algorithm, and the resulting errors were significantly reduced. After applying the neural network, the MVE $\mu_{\Delta X}$ for the X coordinate was equal to 0.00137 m, and the MSE $\sigma^2_{\Delta X}$ was 0.00385 m². MVE $\mu_{\Delta Y}$ was equal to -0.00457 m for the Y coordinate, and MSE $\sigma^2_{\Delta Y}$ was equal to 0.02060 m². For the Z coordinate, MVE $\mu_{\Delta Z}$ was 0.00007 m, and MSE $\sigma^2_{\Delta Z}$ was equal to 0.00004 m². The FO positioning error decreased, MVE $\mu_{\Delta P}$ was equal to 0.12457 m, and MSE $\sigma^2_{\Delta P}$ was equal to 0.00899 m².

If we compare our research results with, for example, the results presented in papers [1] or [25], we can conclude that the combination of the Savitzky-Golay filter and the neural network allows us to reconstruct the FO flight trajectory more effectively and with high accuracy. This method significantly reduces the errors caused by GNSS signal interference and allows reconstruction of the original FO flight trajectory. This approach has great potential for practical applications in aeronautics for processing GNSS signals under jamming conditions

REFERENCES

[1] Hadas, T., Kazmierski, K., & Sośnica, K. (2019). Performance of Galileo-only dual-frequency absolute positioning using the fully serviceable Galileo constellation. *GPS Solutions*, *23*(4), 108.

[2] Rychlicki, M., Kasprzyk, Z., & Rosiński, A. (2020). Analysis of accuracy and reliability of different types of GPS receivers. *Sensors*, *20*(22), 6498.

[3] Nugnes, M., Colombo, C., & Tipaldi, M. (2020). A System-Level Engineering Approach for Preliminary Performance Analysis and Design of Global Navigation Satellite System Constellations. *arXiv preprint arXiv:2009.09387*.

[4] Naciri, N., Yi, D., Bisnath, S., de Blas, F. J., & Capua, R. (2023). Assessment of Galileo High Accuracy Service (HAS) test signals and preliminary positioning performance. *GPS solutions*, *27*(2), 73.

[5] Jansen, P. (2022). *The impact of jamming and spoofing on GNSS signals* (Doctoral dissertation, Delft University of Technology).

[6] Schaefer, M., & Pearson, A. (2021). Accuracy and precision of GNSS in the field. In *GPS and GNSS Technology in Geosciences* (pp. 393-414). Elsevier.

[7] Jiménez-Martínez, M. J., Farjas-Abadia, M., & Quesada-Olmo, N. (2021). An approach to improving GNSS positioning accuracy using several GNSS devices. *Remote Sensing*, *13*(6), 1149.

[8] Hussong, M., Ghizzo, E., Milner, C., Garcia-Pena, A., & Lesouple, J. (2024, September). Characterization of the multipath situation under meaconing interference. In *Proceedings of the 37th International Technical Meeting of the Satellite Division of The Institute of Navigation (ION GNSS+ 2024)* (pp. 3730-3746).

[9] Islam, S., Bhuiyan, M. Z. H., Pääkkönen, I., Saajasto, M., Mäkelä, M., & Kaasalainen, S. (2023, April). Impact analysis of spoofing on different-grade GNSS receivers. In *2023 IEEE/ION Position, Location and Navigation Symposium (PLANS)* (pp. 492-499). IEEE.

[10] Borio, D., & Gioia, C. (2021). GNSS interference mitigation: A measurement and position domain assessment. *NAVIGATION: Journal of the Institute of Navigation*, *68*(1), 93-114.

[11] J Osechas, O., Fohlmeister, F., Dautermann, T., & Felux, M. (2022). Impact of GNSS-band radio interference on operational avionics. *NAVIGATION: Journal of the Institute of Navigation*, *69*(2).

[12] Tsintsadze, G., Manoharan, H., Sahai, A., Beetner, D., & Booth, B. (2024, August). Evaluating Electromagnetic Interference Effects on GNSS Receivers. In *2024 IEEE International Symposium on Electromagnetic Compatibility, Signal & Power Integrity (EMC+ SIPI)* (pp. 308-312). IEEE.

[13] R Brochard, A., Forner, J., Goethal, J., Passeron, T., & Ortega, L. (2024). *Interference modeling and mitigation for GNSS receivers*(Doctoral dissertation, IPSA).

[14] Sun, K., & Zhang, T. (2021). A new GNSS interference detection method based on rearranged wavelet–hough transform. *Sensors*, *21*(5), 1714.

[15] Sun, K., Elhajj, M., & Ochieng, W. Y. (2024). A GNSS Anti-Interference Method based on Fractional Fourier Transform. *IEEE Transactions on Aerospace and Electronic Systems*.

[16] Figuet, B., Waltert, M., Felux, M., & Olive, X. (2022). GNSS Jamming and Its Effect on Air Traffic in Eastern Europe. *Engineering Proceedings*, *28*(1), 12

[17] Silva Lorraine, K. J., & Ramarakula, M. (2023). A comprehensive survey on GNSS interferences and the application of neural networks for anti-jamming. *IETE Journal of Research*, *69*(7), 4286-4305.

[18] van der Merwe, J. R., Contreras Franco, D., Hansen, J., Brieger, T., Feigl, T., Ott, F., ... & Felber, W. (2023). Low-cost COTS GNSS interference monitoring, detection, and classification system. *Sensors*, *23*(7), 3452.

[19] Raichur, N. L., Brieger, T., Jdidi, D., Feigl, T., van der Merwe, J. R., Ghimire, B., ... & Felber, W. (2022, September). Machine learning-assisted GNSS interference monitoring through crowdsourcing. In *Proceedings of the 35th International Technical Meeting of the Satellite Division of The Institute of Navigation (ION GNSS+ 2022), Denver, CO, USA* (pp. 19-23).

[20] Nasser, H., Berz, G., Gómez, M., la Fuente, A. D., Fidalgo, J., Li, W., ... & Troller, M. (2022, September). GNSS interference detection and geolocalization for aviation applications. In *Proceedings of the 35th International Technical Meeting of the Satellite Division of The Institute of Navigation (ION GNSS+ 2022)* (pp. 192-216).

[21] Mehr, I. E., & Dovis, F. (2024). A Deep Neural Network Approach for Classification of GNSS Interference and Jammer. *IEEE Transactions on Aerospace and Electronic Systems*.

[22] Liu, Z., Lo, S., & Walter, T. (2021, September). GNSS interference detection using machine learning algorithms on ADS-B data. In *Proceedings of the 34th International Technical Meeting of the Satellite Division of The Institute of Navigation (ION GNSS+ 2021)* (pp. 4305-4315).

[23] Pérez, A., Querol, J., Park, H., & Camps, A. (2020, September). Radio-frequency interference location, detection and classification using deep neural networks. In *IGARSS 2020-2020 IEEE International Geoscience and Remote Sensing Symposium*(pp. 6977-6980). IEEE.

[24] Wilk, A., Koc, W., Specht, C., Judek, S., Karwowski, K., Chrostowski, P., ... & Szmaglinski, J. (2020). Digital filtering of railway track coordinates in mobile multi–receiver GNSS measurements. *Sensors*, *20*(18), 5018.

[25] Kennedy, H. L. (2020). Improving the frequency response of Savitzky-Golay filters via colored-noise models. *Digital Signal Processing*, *102*, 102743.,

[26] Krasuski, K., Popielarczyk, D., Ciećko, A., & Ćwiklak, J. (2021). A new strategy for improving the accuracy of aircraft positioning using dgps technique in aerial navigation. *Energies*, *14*(15), 4431.

[27] Krasuski, K., Ciećko, A., & Wierzbicki, D. (2022). Accuracy analysis of aircraft positioning using GPS dual receivers in aerial navigation. *Zeszyty Naukowe. Transport/Politechnika Śląska*, (115), 23-34.

[28] Savitzky, A., & Golay, M. J. E. (1964). Smoothing and Differentiation of Data by Simplified Least Squares Procedures. Analytical Chemistry, 36(8), 1627-1639.

[29] Press, W. H., Teukolsky, S. A., Vetterling, W. T., & Flannery, B. P. (2007). Numerical Recipes: The Art of Scientific Computing (3rd ed.). Cambridge University Press.

[30] Hagan, M. T., & Menhaj, M. B. (1994). Training feedforward networks with the Marquardt algorithm. IEEE Transactions on Neural Networks, 5(6), 989-993.

Sebastián Čikovský was born in 1998 in Svidník, Slovak Republic. He received his M.Eng. degree in Aerospace Engineering from the Faculty of Aeronautics, Technical University of Košice, in 2022. Since then, he has been pursuing a Ph.D. degree at the same institution. His research focuses on the impact of interference on Global Navigation SatelliteSystems (GNSS). Areas of interest include GNSS technologies, signal structures of satellite navigation systems, positioning errors in GNSS, the influence of radio-frequency interference on navigation reliability, and advanced methods for GNSS error mitigation and positioning correction algorithms.He is the author of several peer-reviewed scientific papers published in both national and international journals in the field.

Milan Džunda was born in Bardejov, Slovak Republic, in 1956. He received his M.Eng. degree in Aerospace Engineering from the Military Aviation Academy in Košice in 1982, and his CSc. degree (equivalent to Ph.D., Candidate of Technical Sciences) from the Prof. Zhukov Military Aviation Academy in Moscow, Russia, in 1988.

From 1982 to 2005, he held academic positions ranging from Assistant Professor to Head of the Department of Aviation Communication Systems at the Military Aviation Academy in Košice. He is the author of four monographs, more than 150 scientific papers, and one utility model.

His research focuses on the accuracy and resilience of avionics systems against interference. He has served as a principal investigator for multiple research projects funded by the Ministry of Education, Research, Development and Youth of the Slovak Republic.

In 1995, he successfully completed his habilitation at the Military Aviation Academy in Košice and was awarded the academic title of Associate Professor in the field of Measurement Technology. In 1999, he completed his professorship procedure at the same institution and was awarded the academic title of Full Professor in the field of Air Force Armament and Technology.

.